ACS Biomaterials SCIENCE & ENGINEERING

Subscriber access provided by UNIV OF NEWCASTLE

Article

Covalent functionalization of graphene sheets with different moieties and their effects on biological activities

Mohyeddin Assali, Motasem Almasri, Naim Kittana, and Deema Alsouqi

ACS Biomater. Sci. Eng., **Just Accepted Manuscript** • DOI: 10.1021/acsbiomaterials.9b01143 • Publication Date (Web): 10 Dec 2019

Downloaded from pubs.acs.org on December 15, 2019

Just Accepted

"Just Accepted" manuscripts have been peer-reviewed and accepted for publication. They are posted online prior to technical editing, formatting for publication and author proofing. The American Chemical Society provides "Just Accepted" as a service to the research community to expedite the dissemination of scientific material as soon as possible after acceptance. "Just Accepted" manuscripts appear in full in PDF format accompanied by an HTML abstract. "Just Accepted" manuscripts have been fully peer reviewed, but should not be considered the official version of record. They are citable by the Digital Object Identifier (DOI®). "Just Accepted" is an optional service offered to authors. Therefore, the "Just Accepted" Web site may not include all articles that will be published in the journal. After a manuscript is technically edited and formatted, it will be removed from the "Just Accepted" Web site and published as an ASAP article. Note that technical editing may introduce minor changes to the manuscript text and/or graphics which could affect content, and all legal disclaimers and ethical guidelines that apply to the journal pertain. ACS cannot be held responsible for errors or consequences arising from the use of information contained in these "Just Accepted" manuscripts.

is published by the American Chemical Society. 1155 Sixteenth Street N.W., Washington, DC 20036

Published by American Chemical Society. Copyright © American Chemical Society. However, no copyright claim is made to original U.S. Government works, or works produced by employees of any Commonwealth realm Crown government in the course of their duties.

Covalent functionalization of graphene sheets with different moieties and their effects on biological activities

Mohyeddin Assali*[1], Motasem Almasri[2], Naim Kittana[3], Deema Alsouqi[1]

[1] Department of Pharmacy, Faculty of Medicine and Health Sciences, An-Najah National University, P.O.Box 7, Nablus, Palestine.

[2] Department of Biology & Biotechnology, Faculty of Science, An-Najah National University, P.O.Box 7, Nablus, Palestine.

[3] Department of biomedical sciences, Faculty of Medicine and Health Sciences, An-Najah National University, P.O.Box 7, Nablus, Palestine.

Corresponding author: Dr. Mohyeddin Assali

Email: m.d.assali@najah.edu

Tel +970-9-2345113

Fax +970-9-234 9739

Abstract

The ongoing spread of multidrug-resistant bacteria over the past few decades necessitates collateral efforts to develop new classes of antibacterial agents with different mechanisms of action. The utilization of graphene nanosheets has recently gained attention with this respect. Herein, we have synthesized and tested the antibacterial activity of an array of graphene materials covalently functionalized with hydroxyl-, amine-, or carboxyl-containing groups. Fourier transform infrared spectroscopy, and transmission electron microscopy confirmed successful functionalization of the few-layer graphene (FLG). The percentage of weight loss was measured by thermogravimetric analysis, which was found to be 22%, 23%, and 37% for FLG-TEG-OH, FLG-NH_2 and FLG-DEG-COOH, respectively. In comparison with pristine graphene sheets, the functionalized few-layer graphene (*f*-FLG) materials gained an adequate dispersibility in water as confirmed by zeta potential analysis. Moreover, a significant improvement in the antibacterial activity against *Staphylococcus aureus* and *Escherichia coli*, where all *f*-FLG compounds were able to suppress bacterial growth, with a complete suppression achieved by FLG-DEG-COOH. The minimum inhibitory concentration (MIC) was 250 μg/ml for both FLG-TEG-OH and FLG-NH_2, while it was 125 μg/ml for FLG-DEG-COOH. Glutathione oxidation test demonstrated an oxidative stress activity by all *f*-FLG compounds. However, FLG-DEG-COOH demonstrated the highest reduction in glutathione activity. FLG-DEG-COOH and FLG-TEG-OH showed adequate biocompatibility and hemocompatibility. The chemical functionalization of graphene might be a step towards the foundation of an effective class of antimicrobial agents.

Keywords: Diazonium functionalization, water dispersibility, antibacterial, oxidative stress, biocompatibility and hemocompatibility.

1. Introduction

The spread of antibiotic-resistant bacteria is a major worldwide health concern[1-2] that necessitates the development of newer classes of antimicrobial agents with novel characteristics and mechanisms of action. Graphene has recently stepped into the spotlight as a potential antibacterial founder agent, but it is still in the very basic stages.[3]

Graphene has been in the focus of intensive research worldwide since its first isolation in the year 2004.[4] Graphene is formed by a mesh of hexagonal structures of sp^2-hybridized carbon that form two-dimensional (2D) thin sheets of a flat monolayer of carbon atoms that look like a honeycomb. The carbon-carbon distance within graphene sheets is 0.142 nm, while the thickness of the sheets is 1-1.4 nm, and their specific surface area is as high as 2630 $m^2\ g^{-1}$.[5]

Graphene possesses unique materials properties such as excellent thermal conductivity,[6] optical transparency,[7-8] and relatively high electrical conductivity which can readily reach ~10000 $cm^2\ V^{-1}\ s^{-1}$.[9-10] Due to these outstanding properties, graphene has diverse applications in a broad spectrum of technologies like biosensing, solar devices, nanoelectronics, and energy storage.[11-13] However, its biomedical application was challenged by the graphene's low water dispersibility and its tenacious tendency to form aggregates. These hampering challenges could be conquered by non-covalent or covalent functionalization of the surface of the graphene sheets.[14-15] This approach improved the biocompatibility of the functionalized few-layer graphene (*f*-FLG) materials,[16-19] and allowed bioapplications.[20-21] Some of these studies reported that graphene and graphene oxide exhibit effective antimicrobial activity against various types of Gram-negative and Gram-positive bacteria.[22-26] Wang *et al.* reported the antimicrobial activity of three types of graphene derivatives (graphene oxide, fluorinated graphene and guanidine-modified graphene). Their results demonstrated that graphene modified with a guanidine group showed the highest antibacterial activity due to its strong interaction with the bacterial cell membrane.[27] The antimicrobial activity of graphene has been attributed to membrane stress caused by the sharp edges of graphene nanosheets, which might result in physical damages to cell membranes, leading to bacterial lysis.[24, 28-29] Moreover, Liu *et al.* have also reported that the graphene nanomaterials could induce the generation of

reactive oxygen species (ROS) that can be damaging to bacteria. In another study reported by Perreault *et al.* it was found that the antimicrobial activity of graphene sheets is size dependent and is mediated by oxidative mechanisms.[30] By taking the above findings together it becomes promising that the change in the oxidation behavior, size, shape or the functionalization of graphene sheets might affect their antibacterial activity and biocompatibility. However, most of the reported studies focused on suspended graphene nanomaterials in which aggregations may occur and influence their biocompatibility. In addition, the type of functionalization and the surface charges might influence the physicochemical properties of graphene sheets and also the antimicrobial behavior.

Herein, we investigate the effect of covalent functionalization of few layers of graphene sheets, with various functional groups, on the antimicrobial activity using as models Gram-positive (*Staphylococcus aureus*) and Gram-negative (*Escherichia coli*) bacteria as shown in Scheme 1. We have also investigated the possible mechanism of antibacterial activity, as well as biocompatibility of graphene materials.

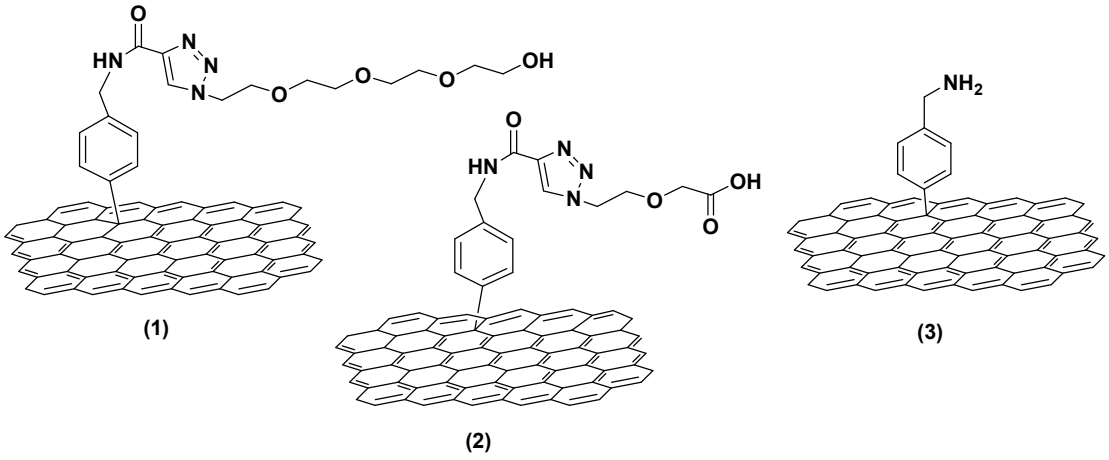

Scheme 1. Covalent functionalization of graphene sheet; (1) FLG-TEG-OH, (2) FLG-DEG-COOH, (3) FLG-NH_2.

2. Experimental section

2.1. Materials and instrumentations

Details regarding the materials and instruments are in the supporting information.

2.2. Synthesis

2.2.1. Synthesis of N-(4-nitrobenzyl) propiolamide (1):

p-nitrobenzyl amine (200 mg, 1.06 mmol), propiolic acid (72 µl, 1.17 mmol), TBTU (375.0 mg, 1.17 mmol) DIPEA (555 µl, 3.18 mmol) and DCM (12 ml) were stirred overnight at room temperature under argon. The crude products were then extracted with dichloromethane (60 ml) followed by a washing step with 30 ml of solution of 1M HCl. The extracted product was dried over anhydrous sodium sulfate. Then it was purified using column chromatography with a mobile phase composed of Hex: EtOAc (1:2) to yield the product (1) (175 mg, 81%) as a yellowish powder. R_f: 0.5 (Hex: EtOAc) (1:2). ^{1}H NMR (500 MHz, $CDCl_3$): δ 8.20 (d, 2H, *J* = 4.9 Hz, Ph), 7.44 (d, 2H, *J* = 4.8 Hz, Ph), 6.42 (bs, 1H, NH), 4.57 (d, 2H, *J* = 5.9 Hz, C$\underline{H_2}$NH), 2.84 (s, 1H, C≡CH). ^{13}C NMR (125.7 MHz, $CDCl_3$): δ 159.0, 152.3, 147.6, 128.4, 124.1, 75.4, 74.4, 43.1.

2.2.2. Reduction for N-(4-aminobenzyl) propiolamide (2):

Zinc powder (504 mg, 7.7 mmol), and ammonium chloride (100 mg, 1.88 mmol) were added to a solution of compound 1 (175 mg, 0.86 mmol) dissolved in a mixture of methanol: water (2:1), and stirred under reflux for 4 h. Then, the reaction was filtrated using silica, washed with ethyl acetate and evaporated to yield a yellowish product with a yield of 95% (142mg). R_f: 0.36 (Hex/EtOAc 1:1). ^{1}H NMR (500 MHz, $CDCl_3$): δ 7.28 (t, 1H, *J* = 7.8 Hz, NHCO), 7.08 (d, 2H, *J* = 8.8 Hz, Ph), 6.64 (d, 2H, *J* = 8.5 Hz, Ph), 5.63 (s, 2H, NH_2), 4.38 (d, 2H, *J* = 5.6 Hz, C$\underline{H_2}$NH), 3.72 (s, 1H, C≡CH). ^{13}C NMR (125.7 MHz, $CDCl_3$): δ 148.4, 145.2, 130.9, 129.3, 129.0, 115.3, 73.2, 72.2, 43.4.

2.2.3. Synthesis of FLG-alkyne (3):

Compound 2 (170 mg, 0.98 mmol) was added to graphene powder (40 mg) under vacuum. 1,2-dichlorobenzene (*o*-DCB) (13 ml) and acetonitrile (7 ml) were added, and

the reaction was sonicated for 10 minutes under argon. Followed by dropwise addition of isoamyl nitrite (786 µl, 5.86 mmol) and stirred overnight at 60 °C. The large unreacted graphene aggregates were removed by low-speed centrifugation at 3000 rpm for 5 min. After that, high-speed centrifugation at 15,000 rpm for 10 min was performed followed by washing with MeOH (2 × 30 ml), DCM (2 × 30 ml) and Et_2O (2 × 30 ml). The product was collected with diethyl ether and dried under reduced pressure. Dry black powder (39 mg) was obtained. Further purification steps were applied after performing click reaction with the various polar linkers that increased the polarity of the graphene sheets, which permitted the separation of the unreacted hydrophobic graphene from the various polar functionalized graphene sheets as shown in the following sections.

2.2.4. Synthesis of OH-TEG-OTs (4):

Tetraethylene glycol (3 g, 15.45 mmol) and triethylamine (2.6 ml, 18.54 mmol) were dissolved in THF (50 ml) and stirred for 5 min at 0 ^{0}C, after that tosyl chloride (2.9 g, 15.45 mmol) was added gradually over a period of 30 min and stirred vigorously overnight at room temperature. The product was extracted with dichloromethane (100 ml × 2), saturated NaCl (50 ml) and dried over anhydrous sodium sulfate, followed by decantation and evaporation under vacuum. The crude product was purified by column chromatography with a mobile phase composed of dichloromethane: methanol (20:1) to obtain an oily product (4) of yield (1.3 g, 26%). R_f: 0.52 (DCM: MeOH) (20:1). ^{1}H NMR: (500 MHz, $CDCl_3$): δ 7.76 (d, 2H, *J* = 8.5 Hz, Ts), 7.35 (d, 2H, *J* = 7.9 Hz, Ts), 4.12 (t, 2H, *J* = 5.4 Hz, CH_2OTs), 3.68-3.55 (m, 14H, 6CH_2O, C$\underline{H_2}$OH), 2.40 (s, 3H, CH_3). ^{13}C NMR (125.7 MHz, $CDCl_3$):δ144.8, 133.0, 129.8, 128.0, 72.5, 70.7, 70.6, 70.4, 70.3, 69.3, 68.7, 61.7, 21.6.

2.2.5. Synthesis of OH-TEG-N_3 (5):

The product was synthesized and characterized according to the literature.[31]

2.2.6. Synthesis of FLG-TEG-OH (6):

Ascorbic acid (20 mg, 0.1 mmol), anhydrous copper sulfate (50 mg, 0.31 mmol) were dissolved in distilled H_2O (3 ml), then a sonicated solution of compound 5 (150 mg, 0.68

mmol) and graphene 3 (50 mg) were dispersed in DCM (3 ml) and were stirred at room temperature for 24 h. Taking advantage of the polarity difference between the FLG-TEG-OH and the unreacted graphene, polar solvent MeOH (20 ml) was added and centrifuged for 10 min. at low speed (3,000 rpm) in order to remove the un-reacted non-polar graphene. After that a centrifugation step for 15 min. at high speed 15,000 rpm in order to remove the excess of the reagents, the supernatant was discarded and the precipitate was washed with MeOH (2 × 20 ml) and Et_2O (2 × 20 ml). The product was collected with Et_2O and dried to obtain black powder (40 mg).

2.2.7. Synthesis of OH-DEG-OTs (7):

A mixture of diethylene glycol (DEG) (1 g, 9.4 mmol) and triethylamine (1.3 ml, 9.4 mmol) in DCM (10 ml) was stirred for 5 min and chilled in an ice bath. Tosyl-chloride (1.8 g, 9.4 mmol) was added gradually for 30 min. The reaction was stirred overnight at room temperature. The product was extracted with DCM (100 ml), saturated NaCl (50 ml) and HCl 1M (50 ml). The product was dried over anhydrous sodium sulfate. The crude product was purified by silica column chromatography with a mobile phase of DCM: MeOH (20:1) to obtain a yield of 25% (600 mg) of an oily product. R_f: 0.4 (DCM: MeOH 20:1). ^{1}H NMR (500 MHz, $CDCl_3$): δ 7.76 (d, 2H, J = 8.6 Hz, Ts), 7.31 (d, 2H, J = 8.1 Hz, Ts), 4.14 (t, 2H, J = 3.4 Hz, CH_2OTs), 3.64 (t, 4H, J = 4.1 Hz, $2CH_2O$), 3.49 (t, 2H, J = 2.1 Hz, $C\underline{H_2}OH$), 2.40 (s, 3H, CH_3). ^{13}C NMR (125.7 MHz, $CDCl_3$): δ 145.0, 142.0, 129.2, 127.9, 72.3, 69.2, 68.6, 61.6, 21.6.

2.2.8. Synthesis of OH-DEG-N_3 (8):

Sodium azide (120 mg, 1.85 mmol) was added to a solution of OH-DEG-OTs 7 (400 mg, 1.54 mmol) dissolved in ethanol (10 ml). The reaction was stirred and refluxed overnight at 70 ºC. The reaction mixture was evaporated and extracted with Et_2O (100 ml) and saturated NaCl (30 ml). The organic layer was dried over anhydrous sodium sulfate. The resulting product was purified using silica gel chromatography (DCM /MeOH (20:1)) to yield the product (8) (215 mg, 99%). R_f: 0.38 (DCM/MeOH 20:1). ^{1}H NMR (500 MHz, $CDCl_3$): δ 4.18 (t, 2H, J = 5.2 Hz, $C\underline{H_2}OH$), 3.74 (t, 2H, J = 5.9 Hz, $OC\underline{H_2}CH_2OH$), 3.46

(t, 2H, *J* = 6.2 Hz, C$\underline{H_2}$$CH_2N_3$), 1.23 (t, 2H, *J* = 5.8 Hz, CH_2N_3). ^{13}C NMR (125.7 MHz, $CDCl_3$): δ 70.6, 68.3, 50.8, 29.5.

2.2.9. Synthesis of 2-(2-azidoethoxy) acetic acid (9):

Jones reagent (7 ml) was added to a solution of OH-DEG-N_3 8 (250 mg, 1.77 mmol) dissolved in acetone (7 ml), the reaction was stirred for 2 h. Then, isopropyl alcohol was added to the reaction drop by drop until the green color is formed, then it was filtrated by silica gel and washed by DCM and then evaporated to obtain the compound 9 with a yield of 65% (180 mg). R_f: 0.4 (DCM: MeOH 9:1). ^{1}H NMR (500 MHz, $CDCl_3$): δ 4.21 (t, 2H, *J* = 4.6 Hz, CH_2COO), 3.73 (t, 2H, *J* = 5.2 Hz, CH_2O), 3.45 (t, 2H, *J* = 4.6 Hz, CH_2N_3). ^{13}C NMR (125.7 MHz, $CDCl_3$):δ173.1, 70.8, 68.1, 50.7.

2.2.10. Synthesis of FLG-DEG-COOH (10):

Ascorbic acid (30 mg, 0.15 mmol) and anhydrous copper sulfate (75 mg, 0.47 mmol) were dissolved in distilled H_2O (4 ml), then the solution was added to a sonicated solution of compound 9 (150 mg, 1.03 mmol), and graphene 3 (60 mg) dispersed in DCM (4 ml) and was stirred overnight at room temperature. The same purification procedure was done as the synthesis of FLG-TEG-OH, MeOH (20 ml) was added to the reaction before it was sonicated and centrifuged for 10 min. at low speed 3,000 rpm followed by centrifugation for 15 min. at 15,000 rpm. The supernatant was discarded and the black precipitate was washed with MeOH (2 × 20 ml) and Et_2O (2 × 15 ml). The black powder was collected with diethyl ether and dried under vacuum. With this condition, 51 mg of dry black powder was obtained.

2.2.11. Synthesis of FLG-NH-Boc (11):

Graphene powder (45 mg) and 4-[(*N*-Boc)aminomethyl]aniline (120 mg, 0.54 mmol) were dried under vacuum. Then 1,2-dichlorobenzene (*o*-DCB) (15 ml) and acetonitrile (10 ml) were added and sonicated for 10 minutes under argon. Then isoamyl nitrite (435 µl, 3.24 mmol) was added drop-wise and stirred for 24 at 60 °C. The functionalized few-layer graphene was dispersed in methanol and centrifugated at low-speed centrifugation (3,000 rpm) for 10 min. and this process repeated three-time to assure the removal of the

unreacted graphene powder. The collected supernatants were washed with MeOH (2 × 15 ml), DCM (2 × 15 ml) and Et_2O (2 × 15 ml). At the final step, the product was collected with diethyl ether and dried under vacuum. 44 mg of dry black powder was obtained.

2.2.12. Synthesis of FLG-NH_2 (12):

FLG-NH-Boc 11 (44 mg) was dispersed in DCM (9 ml) and sonicated for 5 minutes. After that TFA (7 ml) was added and stirred overnight. The same purification procedure was done as the synthesis of FLG-TEG-OH. Then MeOH (20 ml) was added, sonicated and centrifuged for 10 min. at 3,000 rpm followed by centrifugation for 15 min. at 15,000 rpm. This was followed by washing steps with MeOH (2 × 15 ml), DCM (2 × 15 ml) and diethyl ether (2 × 15 ml). The product was collected with diethyl ether and dried under vacuum to obtain (40 mg) of dry black powder.

Quantitative determination of loaded amine (Kaiser test)

Three solutions of phenol, pyridine and ninhydrin were prepared as documented in the literature.[32]

FLG-NH_2 12 (1.2 mg) was weighed in a small tube. Phenol solution (75 µl), pyridine solution (100 µl) and ninhydrin solution (75 µl) were added to the tube. The blank was prepared exactly with the same quantities of solvents but without the FLG-NH_2.[32] The resulting dispersion was sonicated for 5 min. and heated for 10 minutes at 120 °C. The suspension was cooled and diluted with 60% ethanol (1 ml) and filtered by cottoned glass dropper. The tube was washed with 60% ethanol (2 × 0.5 ml). After that, the filtrate was analyzed by UV spectroscopy. The absorbance at λ = 570 nm was correlated to the amount of free amine functions on the graphene surface using the equation:

Concentration (mmol) = (A *d * 10^3) / (extinction coefficient * wt.)

Where A: absorbance of the sample, d: dilution, extinction coefficient: 15000 m^{-1} cm^{-1}, wt.: weight of FLG-NH_2 12.

2.2.13. Glutathione experiment

Following a documented procedure,[33] the glutathione experiment was conducted as follows: graphene derivatives (FLG-TEG-OH 6, FLG-DEG-COOH 10, FLG-NH_2 12) (225 µl at 100 µg/ml) dispersed in 50 mM $NaHCO_3$ buffer (pH 8.6) were mixed with 225 µl of (GSH) (0.8 mM in the $NaHCO_3$ buffer). All samples were prepared in duplicate. The mixtures were transferred into eppendorfs and they were incubated on a shaker at 250 rpm for 2 h protected from light. Then, 15 µl Ellman's reagent and 785 µl of 0.05 M Tris-HCl[34] were added to produce a yellow product. After that, the solution was filtered through a 0.45 µm filter. The absorption was measured for an aliquot of each sample at 405 nm. A sample without graphene was utilized as a negative control. A sample with H_2O_2 (10 mM) was used as a positive control. The loss of (GSH) activity was measured as follow: loss of (GSH %) = (abs. of negative control − abs. of sample)/abs. of negative control) × 100%.

2.3. Determination of antimicrobial activities

2.3.1. Media preparation

Details of media preparation can be found in the supporting information.

2.3.2. Bacterial strains

The antimicrobial activity of graphene compounds was studied against *Escherichia coli* (ATCC® 25922™) and *Staphylococcus aureus* (ATCC® 25923™) strains in comparison with the activity of graphene and normal saline solution.

2.3.3. Preparation of the bacterial suspension

From a fresh culture plate where the bacteria was in the log growth phase according to the Clinical & Laboratory Standards Institute (CLSI) protocol, [35-37] 3 to 4 colonies were transferred to sterile normal saline solution. The turbidity of the bacterial suspension was adjusted to be equivalent 0.5 McFarland standard solution. The 0.5 McFarland standard solution was prepared by mixing 0.5 mL of 1.175% (w/v) $BaCl_2 \cdot 2H_2O$ and 99.5 mL of 1% (v/v) H_2SO_4. Then, the absorbance of the suspension was measured on a

spectrophotometer at λ 630 nm, distilled water was used as the standard blank, to obtain turbidity within 0.08 - 0.1 that reflect the bacterial concentration of about 1.5×10^8 CFU/ml. The McFarland solution was sealed tightly to prevent evaporation and foiled with aluminum foil to protect it from light.

2.3.4. Agar diffusion disk- and well-variant methods

Both methods were utilized as a primary technique to determine the antimicrobial activities of graphene derivatives.[35-36] The plates were sub-cultured with bacteria from the bacterial suspension with a concentration of 1.5×10^8 CFU/ml. In the agar diffusion disk-variant method, small filter paper disks were placed on inoculated plates. This was followed by the addition of 20 µl of the examined compound solution (0.5 mg/ml) on paper disks. On the other hand, agar diffusion well-variant methods involved making wells in agar to which 100 µl of the test compound was added. After the drying of the wells and disk, the plates were incubated at 37 °C for 24 hours. In both methods, each compound was examined in duplicate.

2.3.5. Reduction in bacterial growth

Fresh bacterial cells suspensions (1.5×10^8 CFU/ml) were diluted in a sterile 0.9% normal saline to 10^6 CFU/ml. Graphene derivatives were prepared as a stock solution of 0.5 mg/ml in sterile 0.9% NaCl within 12 hours prior to the antimicrobial experiment. 500 µl was mixed with an equal volume of diluted bacterial suspension and the final concentration of graphene derivative was 250 µg/ml and incubated for 3 hours under constant agitation at room temperature. In parallel, normal saline without graphene derivatives was used as a positive control of bacterial growth. At the end of the period of exposure, a serial dilution was prepared by using a sterile 0.9% NaCl solution. Then 100 µl of each dilution was placed on nutrient agar media immediately. The plates were incubated overnight at 37 °C and the bacterial colonies were counted on the next day.

2.3.6. Broth microdilution method

This method was used in order to measure the minimum inhibitory concentration (MIC) for each graphene derivative. The used procedure was according to the CLSI protocol.[35-

[37] Graphene derivatives were dissolved in 0.9% NaCl to achieve a concentration of 250 µg/ml. McFarland concentration of *S. aureus* and *E. coli* were prepared by using LB broth and diluted to 10^7 CFU/ml. LB broth (100 µl) was filled in each well of 96-well plate and the graphene derivatives were serially diluted (twofold) 11 times. Then 1 µl of bacterial suspension (10^7 CFU/ml) was added to each well except number 11 (negative control). After inoculation of bacteria, the plates were incubated for (18-24) hours at 35 °C. Broth microdilution method was performed in duplicate for each compound. The lowest concentration of each compound that did not allow any visible bacterial growth in the inoculated wells was considered as the minimal inhibitory concentration (MIC).

2.4. Hemolysis assay

A fresh blood sample was collected with heparinized tubes for testing the hemolytic activity and hemocompatibility of synthesized graphene derivatives.[38] Centrifugation at 1000 rpm for 20 min at 4 °C was done for the sample to obtain Human Red Blood Cells (HRBC), the supernatant discharged and washed five times with PBS. HRBCs were diluted 10 times with PBS buffer. Positive control (complete hemolysis) was prepared by incubating H_2O (1 ml) with HRBC suspension (100 µl). Negative control (no hemolysis) was also prepared by incubating PBS (1 ml) and HRBC suspension (100 µl). For the hemolytic activity of the prepared graphene derivatives, HRBC suspension (100 µl) was incubated with (1 ml) of various concentrations of graphene derivatives suspensions (0.2, 0.4 and 0.6 mg/ml in PBS) as testing samples. After gentle shaking, the mixtures were incubated at room temperature in duplicate for 2 and 24 hours. The tubes were centrifuged at 5000 rpm for 1 min. The absorption of the supernatants was read at 541 nm.

The hemolysis percentage was measured as follow:

% of Hemolysis = (abs. of sample – abs. of negative control)/ (abs. of positive control – abs. of negative control)

2.5. Biocompatibility test

HeLa cells were seeded in 96-well plate at a density of 5,000 cells/well. They were supplied with a growth medium composed of DMEM high glucose, 1% v/v L-glutamine, 10% v/v fetal bovine serum and 1% v/v penicillin/streptomycin. All of these reagents were purchased from Biological Industries, Jerusalem. The cells were kept in a cell culture incubator that provided 37 °C, 5% CO_2, and 95% humidity. After 24 h, the medium was exchanged with 100 µl/well of fresh medium containing different concentrations of the test compounds including a blank growth medium as a negative control. After 24 h, 10 µl/well of MTS solution was added and the cells were incubated for 1 h in the cell incubator before the absorbance of the supernatant was measured by a plate reader at a wavelength of 490 nm.

3. Results and discussion

3.1. Synthesis and functionalization of the few-layer graphene sheets

Graphene is hydrophobic and tends to aggregate and precipitate easily in aqueous physiological media. Herein, we aim to functionalize the graphene sheets with three different functional groups using diazonium functionalization[39] to enhance its water dispersibility and study the effect of these functional groups on their antibacterial behavior.

Graphene sheets were firstly functionalized with alkyne group through a multi-stage process, started by reacting, *p*-nitrobenzyl amine with propiolic acid in the presence of TBTU as a coupling agent and DIPEA as Hünig's base to produce compound **1** in a good yield. After that, the nitro group was reduced using zinc and ammonium chloride to obtain the amine compound **2**. In the final step, a diazonium functionalization with compound **2** was achieved in the presence of isoamyl nitrite/*o*-DCB to produce FLG-alkyne **3** in a high yield as shown in scheme 2.

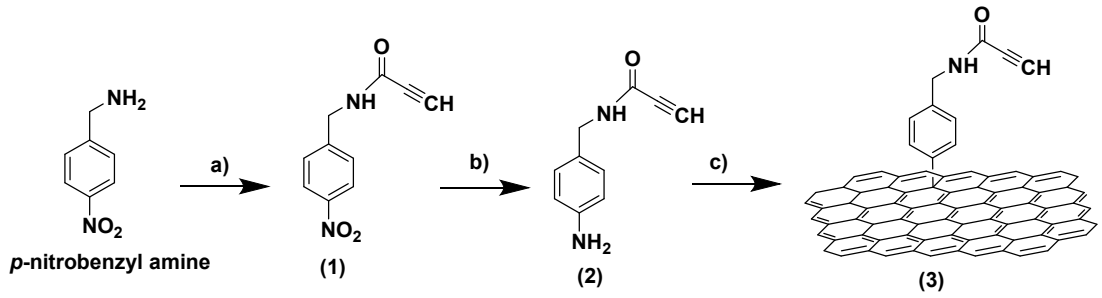

Scheme 2. Synthesis of FLG-alkyne **3**. a) propiolic acid, TBTU, DIPEA; b) Zn and NH_4Cl; c) pristine graphene, isoamyl nitrite, *o*-DCB/CH_3CN.

FLG-alkyne **3** was used as a starting material to obtain the functionalized FLG-TEG-OH and FLG-DEG-COOH. Synthesis of FLG-TEG-OH was undertaken by synthesizing the suitable linker. Beginning with monotosylation of tetraethylene glycol followed by its reaction with sodium azide to obtain OH-TEG-N_3 **5**. Using the advantage of click reaction,[40] FLG-alkyne **3** was clicked with OH-TEG-N_3 **5** in the presence of copper sulfate and sodium ascorbate in DCM/H_2O to produce FLG-TEG-OH in a high yield as shown in scheme 3.

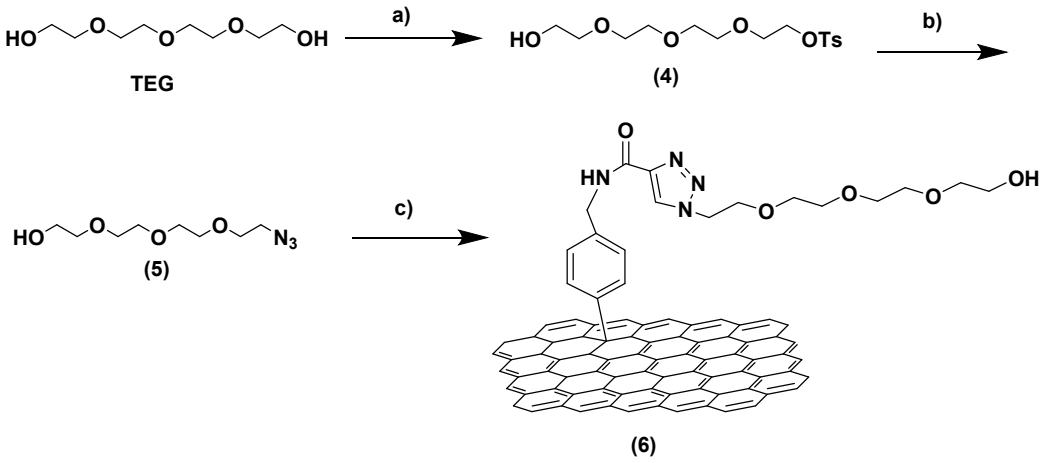

Scheme 3. Synthesis of FLG-TEG-OH **6**. a) Tosyl chloride, Et_3N, DCM; b) NaN_3, ethanol; c) FLG-alkyne 3, $CuSO_4$, sodium ascorbate in DCM:H_2O.

Synthesis of FLG-DEG-COOH was started by monotosylation of diethylene glycol (DEG) through its reaction with tosyl chloride to obtain OH-DEG-Ts linker **7**. After that, the tosylate was replaced by using sodium azide in ethanol to get OH-DEG-N_3 linker **8**, and then oxidized by John's reagent to produce the COOH-DEG-N_3 linker **9**. Finally,

FLG-alkyne **3** was linked with linker **9** through click reaction to obtain FLG-DEG-COOH **10** as shown in scheme 4.

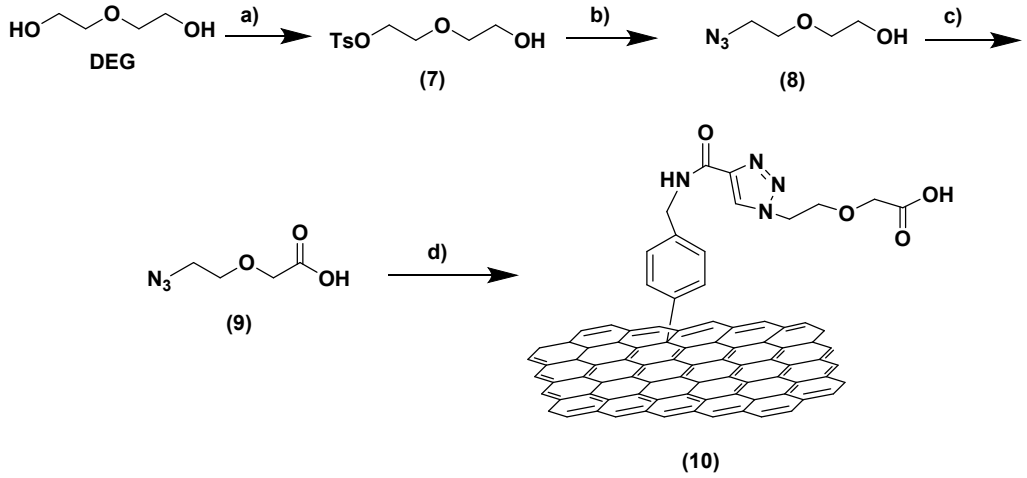

Scheme 4. Synthesis of FLG-DEG-COOH **10**. a) Tosyl chloride, Et_3N, DCM; b) NaN_3, ethanol; c) Jones reagent in acetone; d) FLG-alkyne 3, $CuSO_4$, sodium ascorbate in DCM:H_2O.

The synthesis of FLG-NH_2 was done through the direct diazonium functionalization of graphene sheets with 4-[(*N*-Boc)aminomethyl]aniline through in presence of *o*-DCB, acetonitrile and isoamyl nitrite to get FLG-NHBoc **11**. To obtain the free amine; a deprotection reaction was conducted to remove the Boc group in the presence of trifluoroacetic acid in DCM to obtain FLG-NH_2 **12** as shown in scheme 5. In order to determine the free NH_2 loaded, Kaiser test was conducted obtaining the total amine loaded was 0.72 mmol per gram of graphene.

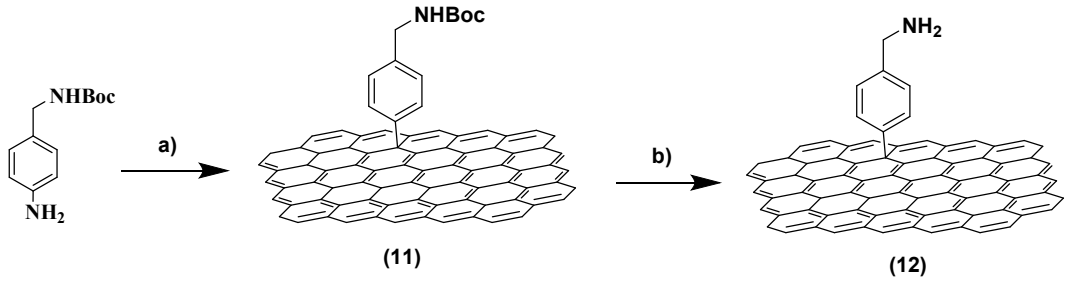

Scheme 5. Synthesis of FLG-amine **12**. a) Pristine graphene, isoamyl nitrite, *o*-DCB/CH_3CN; b) trifluoroacetic acid in DCM.

In order to confirm the presence of the different functional groups, infrared spectra were conducted of the three functionalized graphene (FLG-TEG-OH **6**, FLG-DEG-COOH **10**, and FLG-NH_2 **12**). As can be observed in figure 1, the spectrum of FLG-DEG-COOH confirms the presence of the carboxyl group as the broadband at 3500 cm^{-1} refers to the OH group. The sharp peak at 1730 cm^{-1} and moderate stretch peak at 1260 cm^{-1} refer to the carbonyl group. The stretch peaks at 2925 and 2875 cm^{-1} belong to the methylene groups. Moreover, the moderate stretch peak at 1440 cm^{-1} refers to C=C of the aromatic ring. In addition, the sharp peak at 1100 cm^{-1} refers to the C-O of the ether group. Regarding the FLG-TEG-OH spectrum, the broad peak at 3410 cm^{-1} proves the existence of the alcohol group. The moderate peak at 1350 cm^{-1} refers to the C=C of the aromatic ring and the sharp stretch peak at 1070 cm^{-1} belongs to the C-O of ether. Finally, the sharp peak at 3660 cm^{-1} in the spectrum of FLG-NH_2 confirms the presence of the amine group. The peaks of 2980 and 2890 cm^{-1} refer to the CH of methylene groups and the moderate peak at 1500 cm^{-1} refers to the C=C of the aromatic ring.

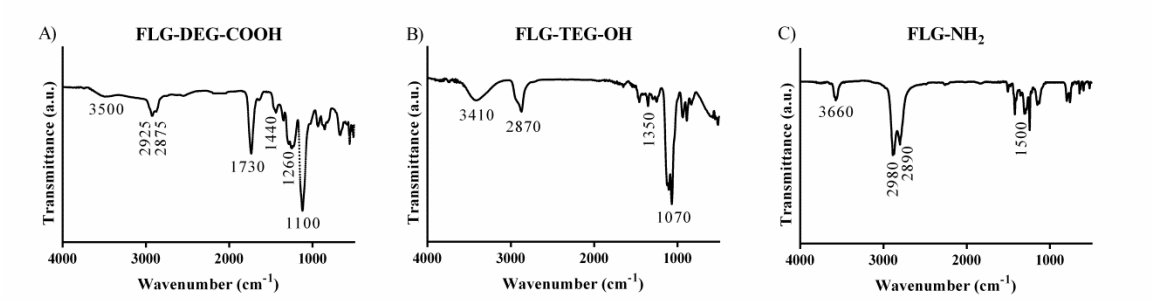

Figure 1. FTIR spectra of A) FLG-DEG-COOH **10**, B) FLG-TEG-OH **6** and C) FLG-NH_2 **12**.

3.2. Dispersibility, stability & Morphology of *f*-FLG

Graphene sheets are considered hydrophobic in character and have low water dispersibility with a high degree of aggregations due to van der Waals interactions between the sheets as shown in figure 2 A.I. Moreover, the transmission electron microscope (TEM) image demonstrates the aggregations of the graphene sheets (figure 2 A.II). However, upon their functionalization with the different functional groups, the graphene becomes more dispersed in water for a whole week and resuspended after performing a sonication for 10 minutes as shown in figure 2 (B.I, C.I, D.I). In addition,

the TEM images of the three different functionalized graphene demonstrate the separation of the graphene sheets and it can be observed few layers of graphene with a diameter range from 0.6-0.8 μm as shown in figure 2 (B.II, C.II, D.II). Liu *et al.* and Perreault *et al.* reported that the larger the lateral size of the graphene sheets as in our case, the stronger would be the obtained antimicrobial activity in comparison to the smaller graphene sheets.[30, 41] Moreover, Russier *et al.* showed that the larger graphene sheets normally have better cellular biocompatibility and can better isolate the cells from their environment.[42]

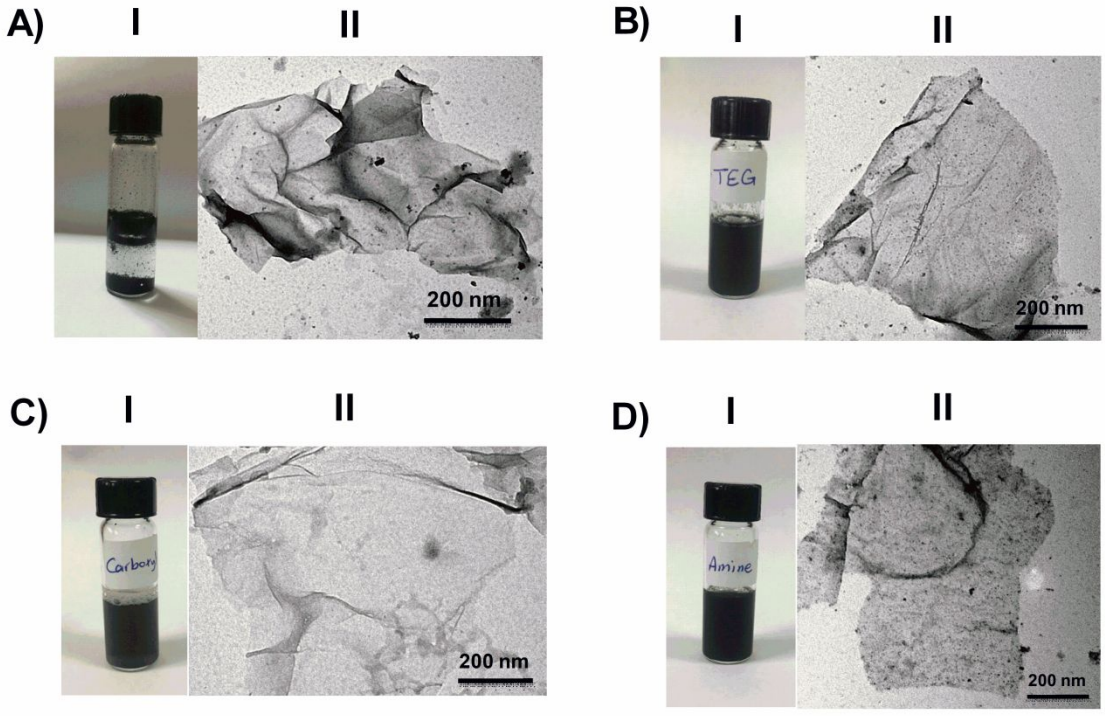

Figure 2. **A) I.** Photograph showing a vial of graphene in water, **II.** TEM image of graphene. **B) I.** Photograph showing a vial of FLG-TEG-OH **6** in water, **II.** TEM image of FLG-TEG-OH **6**. **C) I.** Photograph showing a vial of FLG-DEG-COOH **10** in water, **II.** TEM image of FLG-DEG-COOH **10**. **D) I.** Photograph showing a vial of FLG-NH_2 **12** in water, **II.** TEM image of FLG-NH_2 **12**.

In this study, zeta potential analysis was used to investigate the stability of the *f*-FLG compounds in 0.9% NaCl (*figures S1-S3*). The results obtained showed adequate stability in the case of FLG-DEG-COOH and FLG-TEG-OH with zeta potential of −42.3 and

−30.0 mV, respectively. While FLG-NH_2 showed lesser stability with a zeta potential of +20.2 mV. This relatively high stability might be attributed to the charge repulsion between the carboxylate or hydroxyl groups. This stability could also enhance the antimicrobial activity of these functionalized graphene sheets as reported previously by Karahan *et al*.[43]

3.3. Thermogravimetric analysis

Thermogravimetric analysis was conducted in order to determine the percentage of the weight loss in the functionalized FLG. The mass loss of the functionalized FLG was compared with graphene alone at 700 °C as shown in figure 3. As can be observed, graphene alone is a thermo-stable material and can only lose less than 10% of its weight. However, FLG-TEG-OH **6** showed a weight loss of 32% and approximately the same degree was obtained in the case of FLG-NH_2 **12** (33%). While FLG-DEG-COOH **10** gave the highest degree of functionalization with a percentage of 47%. Excluding the weight loss of the graphene alone, the effective percentage would be 22%, 23% and 37% for FLG-TEG-OH **6**, FLG-NH_2 **12** and FLG-DEG-COOH **10** respectively. As seen, the percentage of weight loss is proportional to the amount of the added functional groups on the surface of the graphene sheets. Moreover, the TGA analysis confirms the successful functionalization of the graphene sheets quantitatively.

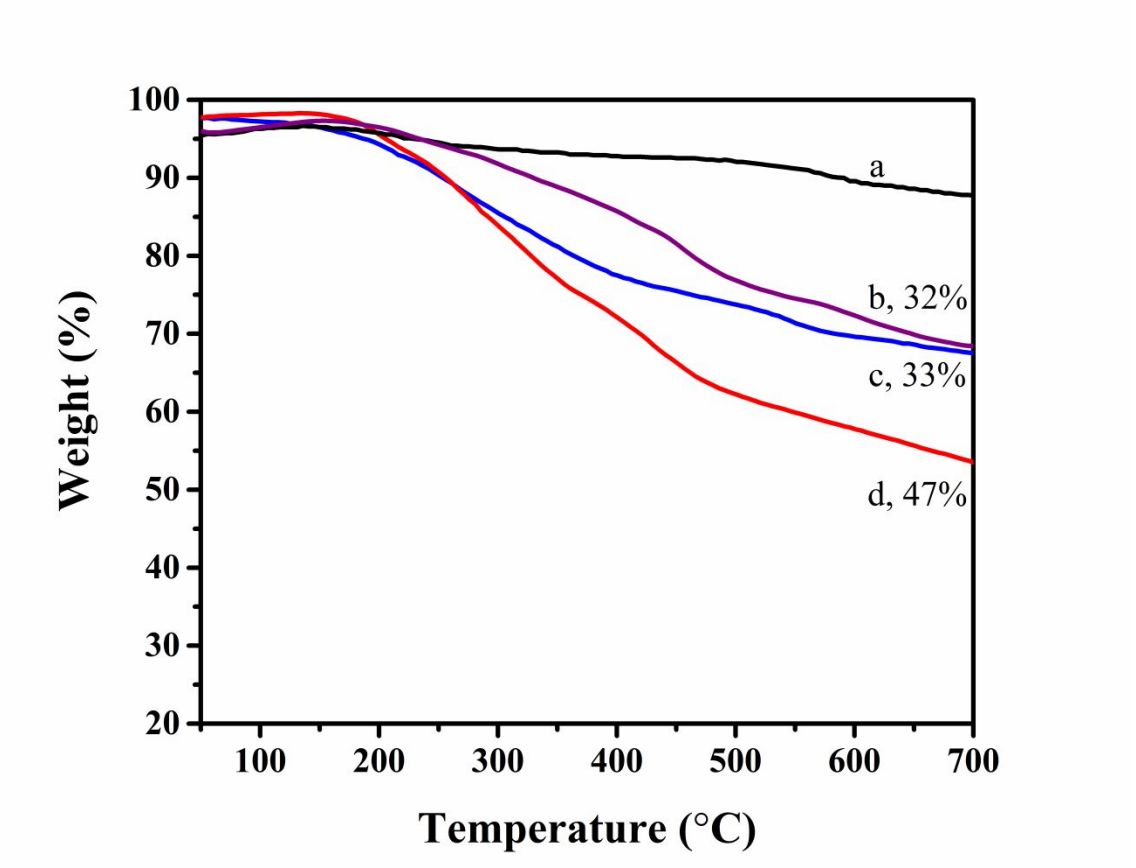

Figure 3. TGA analysis of (a) pristine graphene, (b) FLG-TEG-OH **6**, (c) FLG-NH_2 **12**, (d) FLG-DEG-COOH **10**.

3.4. Antimicrobial activity

As mentioned previously graphene sheets have shown an interesting antimicrobial activity. Herein, we aim to study the effect of the various functionalized graphene (FLG-TEG-OH **6**, FLG-DEG-COOH **10**, and FLG-NH_2 **12**) on their antimicrobial activity. The antibacterial activity was tested on two different bacteria strains (*S. aureus* and *E. coli*) using different techniques such as the agar diffusion disk, the reduction of the colony-forming units and the determination of the minimum inhibitory concentration (MIC). Firstly the disc diffusion technique was performed to assess the antimicrobial activity of each functionalized FLG and compare the results qualitatively with the graphene alone. It was observed form the zone of inhibition that there was an improvement in the antimicrobial activity for *f*-FLG over the pristine graphene. The zone of inhibition was determined in a culture of Gram-positive bacteria (*S. aureus*) and Gram-negative bacteria

(*E. coli*). As can be observed in table 1, the enhancement of the antibacterial activity of the three *f*-FLG in comparison to the graphene as the zone of inhibition was increased in all cases.

Table 1. Zone of inhibition determined by disc diffusion method against *E. coli* and *S. aureus* strains for pristine graphene, FLG-TEG-OH 6, FLG-DEG-COOH 10, FLG-NH_2 12.

	Zone of inhibition value in cm			
	Graphene	FLG-TEG-OH	FLG-DEG-COOH	FLG-NH_2
E. coli	0.1	0.3	0.5	0.4
S. aureus	0.1	0.4	0.6	0.3

In order to determine the antimicrobial activity of the functionalized FLG quantitatively, the minimum inhibitory concentration (MIC) was measured using the broth microdilution technique against *E. coli* and *S. aureus* bacterial strains. The MIC values of the graphene and the functionalized FLG were presented in table 2. The results showed that the functionalization of graphene sheets have improved the antimicrobial activity against both tested bacteria with MIC values of 250 µg/ml in the case of FLG-TEG-OH **6** and FLG-NH_2 **12** and 125 µg/ml of FLG-DEG-COOH **10**, while pristine graphene had a MIC of 500 µg/ml.

Table 2: Minimum inhibitory concentration (MIC) against *S. aureus* and *E. coli* for pristine graphene, graphene-DEG-COOH 10, graphene-NH_2 12, graphene-TEG-OH 6.

	MIC (µg/ml)			
	graphene	FLG-DEG-COOH	FLG-NH_2	FLG-TEG-OH
S. aureus	500	125	250	250
E. coli	500	125	250	250

Moreover, the various functionalization was found to influence the antibacterial activity through a reduction in bacterial viability. As shown in figure 4, the incubation of *E. coli* and *S. aureus* with the different types of functionalized graphene compounds at a concentration of 250 μg/ml resulted in a significant reduction in the bacterial growth in comparison with normal saline (negative control) or pristine graphene. FLG-TEG-OH showed a reduction of about 65% for *S. aureus* and 70% for *E. coli*, while with FLG-NH_2 the percentage of reduction was 50% for *S. aureus* and 85% in the case of *E. coli*. The greatest reduction in bacterial growth was observed by FLG-DEG-COOH. Therefore, all of the synthesized and functionalized graphene nanomaterials showed an improvement in the antibacterial activity in comparison to the pristine graphene. Both the amine and carboxyl functionalized graphene showed better antibacterial activity than hydroxyl functionalized graphene. This might be attributed to the possible charge effect, which influences the interaction with the membranes of the bacteria. However, the degree of functionalization could also play a role since the TGA data showed greater values for FLG-DEG-COOH.

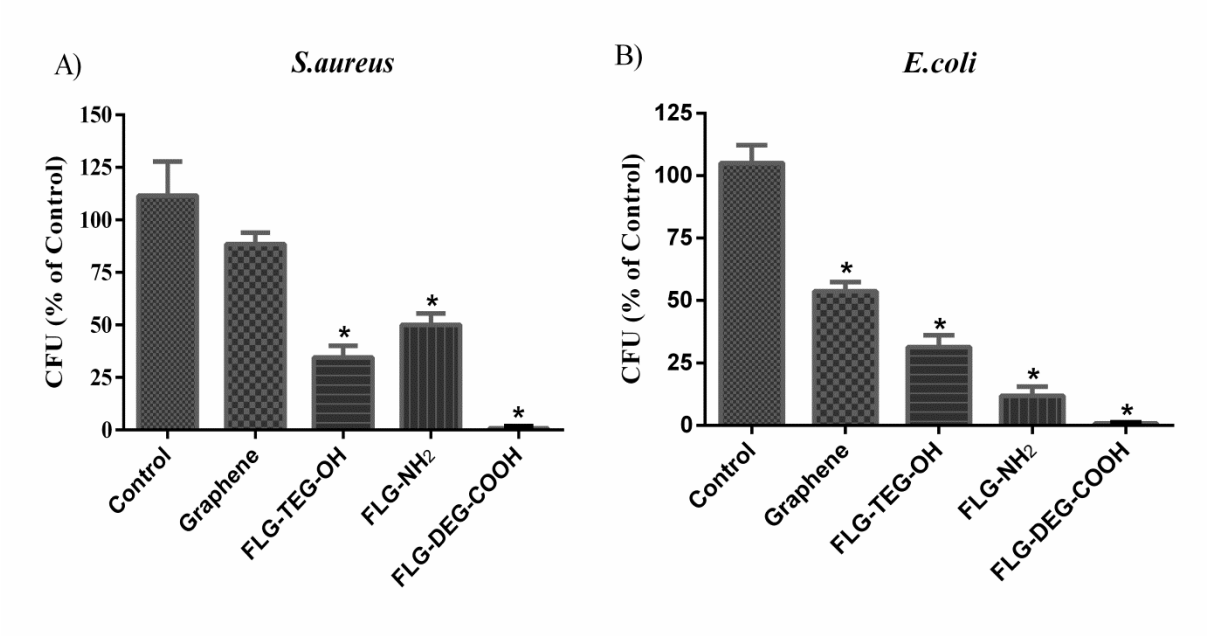

Figure 4. Percentage of CFU reduction of pristine graphene, FLG-TEG-OH 6, FLG-NH_2 12, FLG-DEG-COOH 10 for: A) *S. aureus*, B) *E. coli*. * $p < 0.05$ compared to control determined by student t-test.

In addition, a possible explanation of the antibacterial activity could be referred to the oxidative stress through the generation of free radicals and reactive oxygen species (ROS), which are believed to be able to damage of many cellular components such as DNA, protein and lipids resulting in cell death.[23, 44] However, we cannot exclude the probability of physical disruption of the cell membrane by the direct contact as discussed below.

Herein, we used the glutathione oxidation to investigate the possible oxidative stress-mediated by the various functionalized graphene. Glutathione (GSH) is a tripeptide that contains a thiol group, which has an effective antioxidant activity that shields against the damage of the cellular components by the ROS and free radicals.[45] It is also found in bacteria within millimolar concentration levels to maintain the oxidative balance.[46] Therefore, it can be used as an indicator of the cellular oxidative stress for the carbon nanomaterials.[23, 30, 47] Ellman's assay was used to study the percentage of glutathione activity loss (GSH %) upon exposure to graphene materials.[34] Upon the incubation of the glutathione with the *f*-graphene in bicarbonate buffer the unreacted glutathione was determined by Ellman's reaction (figure 5). As can be observed, a remarkable fraction of the glutathione is oxidized upon the exposure to graphene (27.8%), FLG-TEG-OH (53.5%), FLG-NH_2 (56.7%) and FLG-DEG-COOH (83%). All *f*-FLG showed better loss of glutathione activity in comparison to the graphene alone due to the high generation of oxidative stress, which could explain the improved antibacterial activity of the *f*-FLG nanomaterials. Moreover, the highest percentage in the loss of the glutathione activity was observed by FLG-DEG-COOH, which corresponds to its highest antibacterial activity. Despite the difference in the spacer's length between FLG-NH_2 and FLG-TEG-OH, the oxidative stress activity was very close, which might indicate that the difference in the length of the spacers is not likely to significantly play a role in the antimicrobial activity. This observation is directed to the reactive oxygen species formation with the high oxygen-containing graphene sheets.[48] However, we cannot exclude a role for the physical disruption of the cell membrane by the direct contact between the graphene sheets and the cellular systems which causes destruction of the outer membrane and cell death as evidenced by the pristine graphene in data and in the previous studies by other groups.[30]

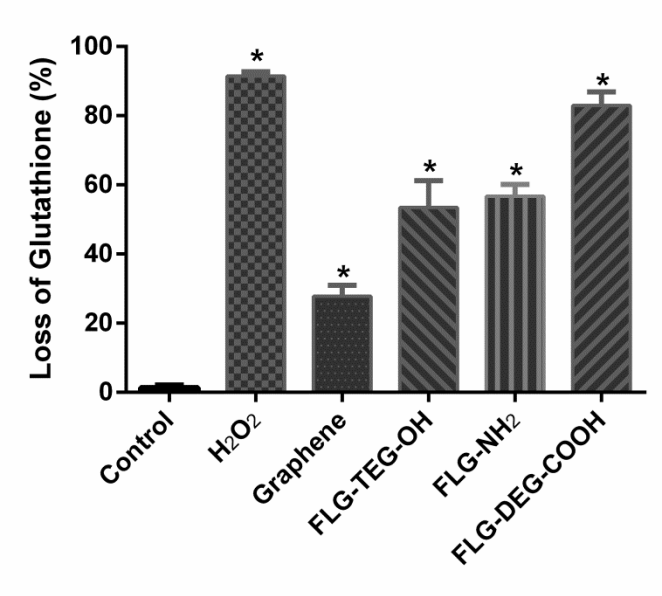

Figure 5. Loss of glutathione (%) by pristine graphene and the *f*-graphene materials. * $p < 0.05$ compared to control, determined by student t-test.

3.5. Hemo-compatibility and biocompatibility of *f*-graphene nanomaterials

One of the important conditions for the application of the nanomaterials *in vivo* is the hemocompatibility, as they are more likely to interact primarily with the red blood cells that can result in hemolysis. In this study, we evaluate the percentage of hemoglobin release from intact fresh red blood cells following incubation with various concentrations (200, 400 and 600 µg/ml) of *f*-graphene nanomaterials over 2 and 24 hours. The permissible percentage of the hemolytic activity should be less than 5% in order for a substance to be considered as hemocompatible.[49] Accordingly as shown in figure 6, graphene, FLG-TEG-OH and FLG-DEG-COOH did not induce significant hemolysis at any of the tested concentrations for up to 24 hours. However, FLG-NH_2 induced a significant concentration-dependent hemolytic activity in the short-term (2 hours) and long-term (24 hours). The reason behind that might be due to the reaction of the amino group with cysteine-β-93 amino acid on hemoglobin as previously reported by another group.[50] It is important to point out that the hemocompatibility test was performed for up to 600 µg/ml. Testing higher concentrations could induce aggregations that are most likely not compatible with blood cells.

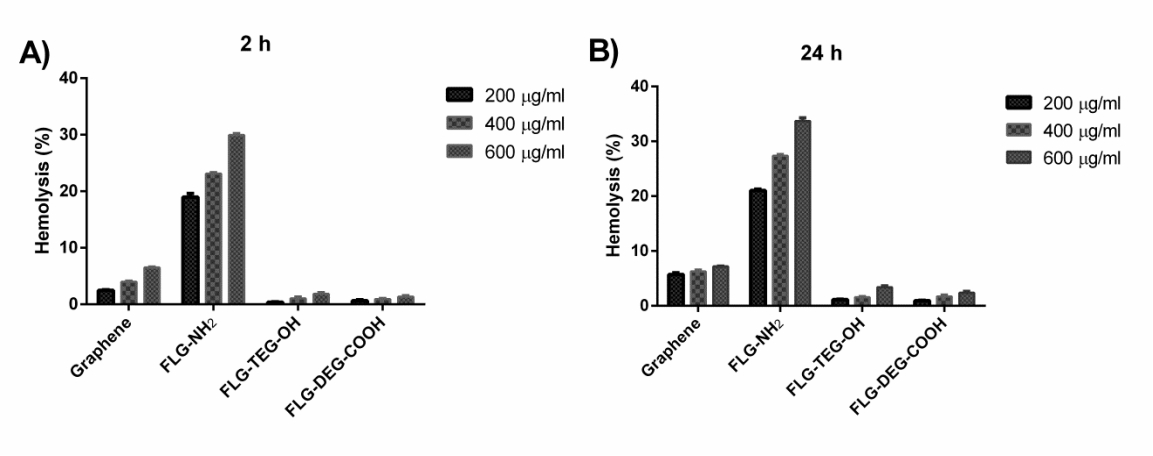

Figure 6. Percentage of hemolysis at three different concentrations (200, 400, and 600 μg/ml) of pristine graphene and *f*-graphene nanomaterials after A) 2 hours and B) 24 hours.

Moreover, the biocompatibility of the different functionalized graphene sheets was tested on HeLa cells. As shown in figure 7, FLG-TEG-OH demonstrated no cytotoxicity within the tested concentration range (0-1250 μg/ml). However, FLG-NH_2 showed adequate biocompatibility only up to 312.5 μg/ml, whereas FLG-DEG-COOH reduced the cell viability by around 10% at 625 and 1250 μg/ml.

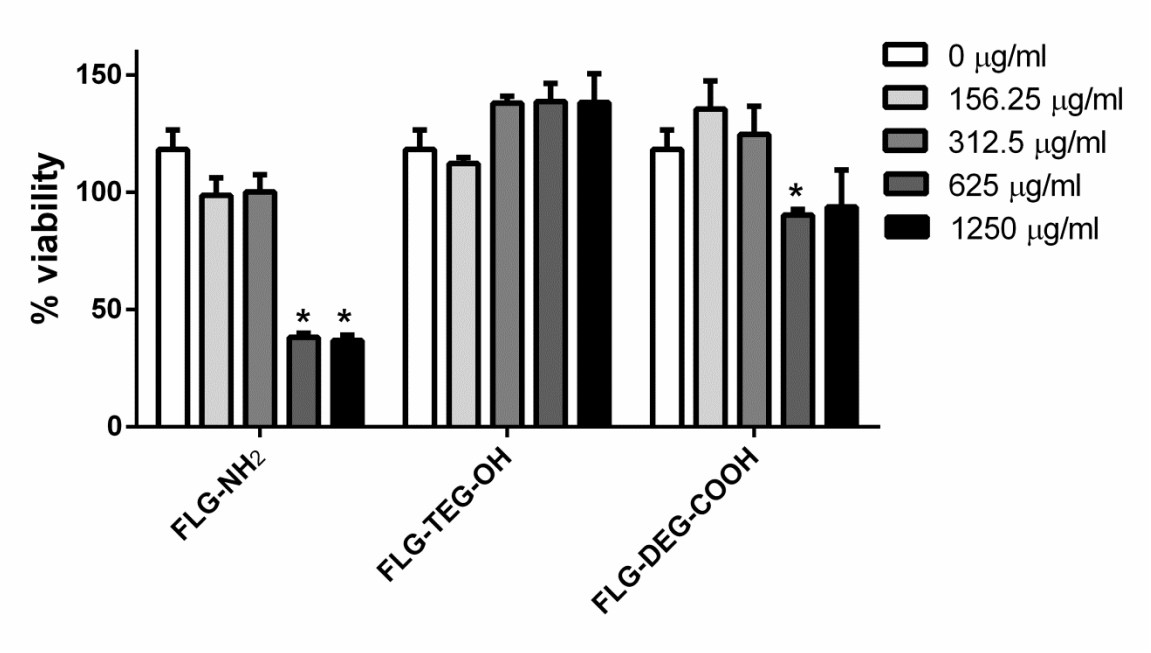

Figure 7. Percentage of HeLa cell viability under treatment with various concentrations (0-1250 μg/ml) of FLG-NH_2, FLG-TEG-OH, and FLG-DEG-COOH.

4. Conclusion

The covalent functionalization of graphene sheets with various functional groups (hydroxyl, amine, or carboxyl) was confirmed by FTIR. The water dispersibility was improved with good stability as evidenced by zeta potential analysis. Moreover, the obtained functionalized graphene nanomaterials were characterized by transmission electron microscope. The percentages of weight loss, determined by TGA, were 22%, 23%, and 37% for FLG-TEG-OH, FLG-NH_2 and FLG-DEG-COOH, respectively. FLG-DEG-COOH showed the highest antibacterial activity with MIC of 125 μg/ml and a complete reduction in the CFU. At the same time, the glutathione oxidation test demonstrated an oxidative stress activity of the functionalized graphene nanomaterials with the highest reduction in the case of FLG-DEG-COOH. Finally, FLG-TEG-OH and FLG-DEG-COOH showed adequate hemo/biocompatibility, which is encouraging for pursuing *in vivo* investigations in the future.

Acknowledgments

The authors acknowledge Dr. Saed Khammash for editing the article. Authors also thank Hamdi Mango Center for Scientific Research and faculty of medicine at the University of Jordan for their collaboration in TEM, NMR, and TGA measurements.

Supporting Information

Reagents, instruments, media preparation, and Zeta potential graphs of the *f*-graphene nanomaterials.

Reference

1. Lushniak, B. D., Antibiotic Resistance: A Public Health Crisis. *Public Health Reports* **2014,** *129* (4), 314-316. DOI: 10.1177/003335491412900402.
2. Bush, K.; Courvalin, P.; Dantas, G.; Davies, J.; Eisenstein, B.; Huovinen, P.; Jacoby, G. A.; Kishony, R.; Kreiswirth, B. N.; Kutter, E.; Lerner, S. A.; Levy, S.; Lewis, K.; Lomovskaya, O.; Miller, J. H.; Mobashery, S.; Piddock, L. J. V.; Projan, S.; Thomas, C. M.; Tomasz, A.; Tulkens, P. M.; Walsh, T. R.; Watson, J. D.; Witkowski, J.; Witte, W.; Wright, G.; Yeh, P.; Zgurskaya, H. I., Tackling antibiotic resistance. *Nature Reviews Microbiology* **2011,** *9* (12), 894-896. DOI: 10.1038/nrmicro2693.
3. Karahan, H. E.; Wiraja, C.; Xu, C.; Wei, J.; Wang, Y.; Wang, L.; Liu, F.; Chen, Y., Graphene Materials in Antimicrobial Nanomedicine: Current Status and Future Perspectives. *Advanced Healthcare Materials* **2018,** *7* (13), e1701406. DOI: 10.1002/adhm.201701406.
4. Novoselov, K. S., Electric Field Effect in Atomically Thin Carbon Films. *Science* **2004,** *306* (5696), 666-669. DOI: 10.1126/science.1102896.
5. Rao, C. N. R.; Sood, A. K.; Subrahmanyam, K. S.; Govindaraj, A., Graphene: The New Two-Dimensional Nanomaterial. *Angewandte Chemie International Edition* **2009,** *48* (42), 7752-7777. DOI: 10.1002/anie.200901678.
6. Balandin, A. A.; Ghosh, S.; Bao, W.; Calizo, I.; Teweldebrhan, D.; Miao, F.; Lau, C. N., Superior Thermal Conductivity of Single-Layer Graphene. *Nano Letters* **2008,** *8* (3), 902-907. DOI: 10.1021/nl0731872.
7. Nair, R. R.; Blake, P.; Grigorenko, A. N.; Novoselov, K. S.; Booth, T. J.; Stauber, T.; Peres, N. M. R.; Geim, A. K., Fine Structure Constant Defines Visual Transparency of Graphene. *Science* **2008,** *320* (5881), 1308-1308. DOI: 10.1126/science.1156965.
8. Kuzmenko, A. B.; van Heumen, E.; Carbone, F.; van der Marel, D., Universal Optical Conductance of Graphite. *Physical review letters* **2008,** *100* (11). DOI: 10.1103/PhysRevLett.100.117401.
9. Morozov, S. V.; Novoselov, K. S.; Katsnelson, M. I.; Schedin, F.; Elias, D. C.; Jaszczak, J. A.; Geim, A. K., Giant Intrinsic Carrier Mobilities in Graphene and Its Bilayer. *Physical review letters* **2008,** *100* (1). DOI: 10.1103/PhysRevLett.100.016602.
10. Chen, J.-H.; Jang, C.; Xiao, S.; Ishigami, M.; Fuhrer, M. S., Intrinsic and extrinsic performance limits of graphene devices on SiO2. *Nature Nanotechnology* **2008,** *3* (4), 206-209. DOI: 10.1038/nnano.2008.58.

11. Lin, Y. M.; Dimitrakopoulos, C.; Jenkins, K. A.; Farmer, D. B.; Chiu, H. Y.; Grill, A.; Avouris, P., 100-GHz Transistors from Wafer-Scale Epitaxial Graphene. *Science* **2010,** *327* (5966), 662-662. DOI: 10.1126/science.1184289.
12. Schedin, F.; Geim, A. K.; Morozov, S. V.; Hill, E. W.; Blake, P.; Katsnelson, M. I.; Novoselov, K. S., Detection of individual gas molecules adsorbed on graphene. *Nature Materials* **2007,** *6* (9), 652-655. DOI: 10.1038/nmat1967.
13. Liao, L.; Bai, J.; Lin, Y.-C.; Qu, Y.; Huang, Y.; Duan, X., High-Performance Top-Gated Graphene-Nanoribbon Transistors Using Zirconium Oxide Nanowires as High-Dielectric-Constant Gate Dielectrics. *Advanced Materials* **2010,** *22* (17), 1941-1945. DOI: 10.1002/adma.200904415.
14. Georgakilas, V.; Bourlinos, A. B.; Zboril, R.; Steriotis, T. A.; Dallas, P.; Stubos, A. K.; Trapalis, C., Organic functionalisation of graphenes. *Chemical Communications* **2010,** *46* (10), 1766. DOI: 10.1039/b922081j.
15. Georgakilas, V.; Otyepka, M.; Bourlinos, A. B.; Chandra, V.; Kim, N.; Kemp, K. C.; Hobza, P.; Zboril, R.; Kim, K. S., Functionalization of Graphene: Covalent and Non-Covalent Approaches, Derivatives and Applications. *Chemical Reviews* **2012,** *112* (11), 6156-6214. DOI: 10.1021/cr3000412.
16. Yang, K.; Feng, L.; Shi, X.; Liu, Z., Nano-graphene in biomedicine: theranostic applications. *Chem. Soc. Rev.* **2013,** *42* (2), 530-547. DOI: 10.1039/c2cs35342c.
17. Yang, K.; Wan, J.; Zhang, S.; Zhang, Y.; Lee, S.-T.; Liu, Z., In VivoPharmacokinetics, Long-Term Biodistribution, and Toxicology of PEGylated Graphene in Mice. *ACS Nano* **2011,** *5* (1), 516-522. DOI: 10.1021/nn1024303.
18. Zhang, S.; Yang, K.; Feng, L.; Liu, Z., In vitro and in vivo behaviors of dextran functionalized graphene. *Carbon* **2011,** *49* (12), 4040-4049. DOI: 10.1016/j.carbon.2011.05.056.
19. Singh, S. K.; Singh, M. K.; Kulkarni, P. P.; Sonkar, V. K.; Grácio, J. J. A.; Dash, D., Amine-Modified Graphene: Thrombo-Protective Safer Alternative to Graphene Oxide for Biomedical Applications. *ACS Nano* **2012,** *6* (3), 2731-2740. DOI: 10.1021/nn300172t.
20. Chung, C.; Kim, Y.-K.; Shin, D.; Ryoo, S.-R.; Hong, B. H.; Min, D.-H., Biomedical Applications of Graphene and Graphene Oxide. *Accounts of Chemical Research* **2013,** *46* (10), 2211-2224. DOI: 10.1021/ar300159f.
21. An, S. S.; Wu, S.-Y.; Hulme, J., Current applications of graphene oxide in nanomedicine. *International Journal of Nanomedicine* **2015**, 9. DOI: 10.2147/ijn.s88285.
22. Li, J.; Wang, G.; Zhu, H.; Zhang, M.; Zheng, X.; Di, Z.; Liu, X.; Wang, X., Antibacterial activity of large-area monolayer graphene film manipulated by charge transfer. *Scientific Reports* **2014,** *4* (1). DOI: 10.1038/srep04359.
23. Liu, S.; Zeng, T. H.; Hofmann, M.; Burcombe, E.; Wei, J.; Jiang, R.; Kong, J.; Chen, Y., Antibacterial Activity of Graphite, Graphite Oxide, Graphene Oxide, and Reduced Graphene Oxide: Membrane and Oxidative Stress. *ACS Nano* **2011,** *5* (9), 6971-6980. DOI: 10.1021/nn202451x.
24. Akhavan, O.; Ghaderi, E., Toxicity of Graphene and Graphene Oxide Nanowalls Against Bacteria. *ACS Nano* **2010,** *4* (10), 5731-5736. DOI: 10.1021/nn101390x.
25. Krishnamoorthy, K.; Veerapandian, M.; Zhang, L.-H.; Yun, K.; Kim, S. J., Antibacterial Efficiency of Graphene Nanosheets against Pathogenic Bacteria via Lipid

Peroxidation. *The Journal of Physical Chemistry C* **2012,** *116* (32), 17280-17287. DOI: 10.1021/jp3047054.
26. Zou, X.; Zhang, L.; Wang, Z.; Luo, Y., Mechanisms of the Antimicrobial Activities of Graphene Materials. *Journal of the American Chemical Society* **2016,** *138* (7), 2064-77. DOI: 10.1021/jacs.5b11411.
27. Wang, X.; Lu, P.; Li, Y.; Xiao, H.; Liu, X., Antibacterial activities and mechanisms of fluorinated graphene and guanidine-modified graphene. *RSC Advances* **2016,** *6* (11), 8763-8772. DOI: 10.1039/c5ra28030c.
28. Hu, W.; Peng, C.; Luo, W.; Lv, M.; Li, X.; Li, D.; Huang, Q.; Fan, C., Graphene-Based Antibacterial Paper. *ACS Nano* **2010,** *4* (7), 4317-4323. DOI: 10.1021/nn101097v.
29. Tu, Y.; Lv, M.; Xiu, P.; Huynh, T.; Zhang, M.; Castelli, M.; Liu, Z.; Huang, Q.; Fan, C.; Fang, H.; Zhou, R., Destructive extraction of phospholipids from Escherichia coli membranes by graphene nanosheets. *Nature Nanotechnology* **2013,** *8* (8), 594-601. DOI: 10.1038/nnano.2013.125.
30. Perreault, F.; de Faria, A. F.; Nejati, S.; Elimelech, M., Antimicrobial Properties of Graphene Oxide Nanosheets: Why Size Matters. *ACS Nano* **2015,** *9* (7), 7226-7236. DOI: 10.1021/acsnano.5b02067.
31. Assali, M.; Zaid, A. N.; Kittana, N.; Hamad, D.; Amer, J., Covalent functionalization of SWCNT with combretastatin A4 for cancer therapy. *Nanotechnology* **2018,** *29* (24), 245101. DOI: 10.1088/1361-6528/aab9f2.
32. E. Kaiser, R. L. C., C. D. Bossinger, and P. I. Cook, *Color test for detection of free terminal amino groups in the solid-phase synthesis of peptides*. 1970; Vol. 34, p 595–598.
33. Vecitis, C. D.; Zodrow, K. R.; Kang, S.; Elimelech, M., Electronic-Structure-Dependent Bacterial Cytotoxicity of Single-Walled Carbon Nanotubes. *ACS Nano* **2010,** *4* (9), 5471-5479. DOI: 10.1021/nn101558x.
34. Ellman, G. L., Tissue sulfhydryl groups. *Archives of Biochemistry and Biophysics* **1959,** *82* (1), 70-77. DOI: 10.1016/0003-9861(59)90090-6.
35. Lorian, V., *Antibiotics in laboratory medicine*. 5th edition ed.; Philadelphia, PA, 2005.
36. CLSI, Performance Standards for Antimicrobial Susceptibility Testing; Twenty-Third Informational Supplement. In *CLSI document M02-A11*, 7th edition ed.; Clinical and Laboratory Standards Institute, 950 West Valley Road, Suite 2500, Wayne ,Pennsylvania 19087, USA, 2012.
37. Balouiri, M.; Sadiki, M.; Ibnsouda, S. K., Methods for in vitro evaluating antimicrobial activity: A review. *Journal of Pharmaceutical Analysis* **2016,** *6* (2), 71-79. DOI: 10.1016/j.jpha.2015.11.005.
38. Thorat, N. D.; Bohara, R. A.; Tofail, S. A. M.; Alothman, Z. A.; Shiddiky, M. J. A.; A Hossain, M. S.; Yamauchi, Y.; Wu, K. C. W., Superparamagnetic Gadolinium Ferrite Nanoparticles with Controllable Curie Temperature - Cancer Theranostics for MR-Imaging-Guided Magneto-Chemotherapy. *European Journal of Inorganic Chemistry* **2016,** *2016* (28), 4586-4597. DOI: 10.1002/ejic.201600706.
39. Lomeda, J. R.; Doyle, C. D.; Kosynkin, D. V.; Hwang, W.-F.; Tour, J. M., Diazonium Functionalization of Surfactant-Wrapped Chemically Converted Graphene Sheets. *Journal of the American Chemical Society* **2008,** *130* (48), 16201-16206. DOI: 10.1021/ja806499w.

40. Kolb, H. C.; Finn, M. G.; Sharpless, K. B., Click Chemistry: Diverse Chemical Function from a Few Good Reactions. *Angew Chem Int Ed Engl* **2001,** *40* (11), 2004-2021. DOI: 10.1002/1521-3773(20010601)40:11<2004::AID-ANIE2004>3.0.CO;2-5 [pii].
41. Liu, S.; Hu, M.; Zeng, T. H.; Wu, R.; Jiang, R.; Wei, J.; Wang, L.; Kong, J.; Chen, Y., Lateral dimension-dependent antibacterial activity of graphene oxide sheets. *Langmuir* **2012,** *28* (33), 12364-72. DOI: 10.1021/la3023908.
42. Russier, J.; Treossi, E.; Scarsi, A.; Perrozzi, F.; Dumortier, H.; Ottaviano, L.; Meneghetti, M.; Palermo, V.; Bianco, A., Evidencing the mask effect of graphene oxide: a comparative study on primary human and murine phagocytic cells. *Nanoscale* **2013,** *5* (22), 11234-47. DOI: 10.1039/c3nr03543c.
43. Karahan, H. E.; Wei, L.; Goh, K.; Wiraja, C.; Liu, Z.; Xu, C.; Jiang, R.; Wei, J.; Chen, Y., Synergism of Water Shock and a Biocompatible Block Copolymer Potentiates the Antibacterial Activity of Graphene Oxide. *Small* **2016,** *12* (7), 951-62. DOI: 10.1002/smll.201502496.
44. Murr, L., Cytotoxicity and reactive oxygen species generation from aggregated carbon and carbonaceous nanoparticulate materials. *International Journal of Nanomedicine* **2008**, 83. DOI: 10.2147/ijn.s2464.
45. Pompella, A.; Visvikis, A.; Paolicchi, A.; De Tata, V.; Casini, A. F., The changing faces of glutathione, a cellular protagonist. *Biochemical Pharmacology* **2003,** *66* (8), 1499-503. DOI: S0006295203005045 [pii].
46. Fahey, R. C.; Brown, W. C.; Adams, W. B.; Worsham, M. B., Occurrence of glutathione in bacteria. *Journal of Bacteriology* **1978,** *133* (3), 1126-9.
47. Vecitis, C. D.; Zodrow, K. R.; Kang, S.; Elimelech, M., Electronic-structure-dependent bacterial cytotoxicity of single-walled carbon nanotubes. *ACS Nano* **2010,** *4* (9), 5471-9. DOI: 10.1021/nn101558x.
48. Liu, X.; Sen, S.; Liu, J.; Kulaots, I.; Geohegan, D.; Kane, A.; Puretzky, A. A.; Rouleau, C. M.; More, K. L.; Palmore, G. T.; Hurt, R. H., Antioxidant deactivation on graphenic nanocarbon surfaces. *Small* **2011,** *7* (19), 2775-85. DOI: 10.1002/smll.201100651.
49. Haghniaz, R.; Bhayani, K. R.; Umrani, R. D.; Paknikar, K. M., Dextran stabilized lanthanum strontium manganese oxide nanoparticles for magnetic resonance imaging. *RSC Advances* **2013,** *3* (40), 18489. DOI: 10.1039/c3ra40836a.
50. Meyer, V. R., Laboratory Profile: Red blood cells and toxic chemicals. *Analytical Chemistry* **1997,** *69* (11), 340A-340A. DOI: 10.1021/ac971651p.

For Table of Contents Use Only

Covalent functionalization of graphene sheets with different moieties and their effects on biological activities

Mohyeddin Assali*[1], Motasem Almasri[2], Naim Kittana[3], Deema Alsouqi[1]